Supporting Information

Task-Specific Tailored Cationic Polymeric Network with High Base-Resistance for Unprecedented ^{99}TcO$_4^-$ Cleanup from Alkaline Nuclear Waste

Jie Li,[#] Baoyu Li,[#] Nannan Shen, Lixi Chen, Qi Guo, Long Chen, Linwei He, Xing Dai, Zhifang Chai, and Shuao Wang*

State Key Laboratory of Radiation Medicine and Protection, School for Radiological and Interdisciplinary Sciences (RAD-X) and Collaborative Innovation Center of Radiation Medicine of Jiangsu Higher Education Institutions, Soochow University, Suzhou 215123, China

* Email: shuaowang@suda.edu.cn

Table of Contents   Page

Section 1. Materials and reagents

1,3,5-Tris(p-formylphenyl)benzene (TFP) and 1,4-bisbenzil were purchased from Jilin Chinese Academy of Sciences-Yanshen Technology Co., Ltd., and Jiangsu Argon xenon Material Technology Co., Ltd., respectively. CH$_3$I, acetic acid (glacial), nitric acid were purchased from the Experimental Materials Supply Center of Suchow University. NaReO$_4$ was purchased from Alfa Aesar (China) Chemical Co., Ltd. Other chemicals like dimethyl sulfoxide (DMSO), dimethyl Formamide (DMF), 1,4-dioxane, ammonium acetate, NaOH, HNO$_3$, NaNO$_3$, Na$_2$SO$_4$, Na$_2$CO$_3$, NaCl, and used in this work were purchased from the supplier in analytical pure (AR) and used without further purification.

Section 2. Synthesis of SCU-CPN-4

SCU-PN. 0.52 g of TFP, 0.682 g of 1,4-bisbenzil, 3.08 g of ammonium acetate, 6 mL of acetic acid (glacial), and 18 mL of 1,4-dioxane were mixed and added into a 50 mL round-bottom flask, after stringing and refluxing the mixture for 24 h, the yellow polymer (SCU-PN) was filtered and washed with 1,4-dioxane, ethanol and deionized water for three times successively.

SCU-MPN. 1 g of SCU-PN, 12 mL of 5 M KOH, and 100 mL of DMSO were mixed and stirred at a 100 mL round-bottom flask with a glass stopper. Then the mixture was heated to 60 °C, 3 mL of 5 M KOH, and 10 mL of DMSO was added additionally. After being stirred at 60 °C for 30 min, the mixture was cooled to room temperature and 1.5 g of iodomethane was added rapidly. After stringing the mixture at room temperature for 12 h, the obtained SCU-MPN was filtered and washed with DMSO, ethanol, and deionized water three times successively.

SCU-CPN-4-I. 1 g of SCU-MPN and 1.5 g of iodomethane were added to 150 ml of DMF at a 250 mL round-bottom flask. After stirring the resulting mixture at 100 °C for 24 h, the obtained SCU-CPN-I was filtered and washed with three times of DMF, ethanol, and deionized water successively.

SCU-CPN-4. SCU-CPN-4 was obtained after soaking SCU-CPN-4-I powders with saturated sodium chloride (NaCl) solution three times.

Section 3. Characterizations

The prepared SCU-CPN-4 materials were characterized by FT-IR (Fourier Transform Infrared Spectroscopy), SEM (Scanning Electron Microscope), TEM-EDS (Transmission Electron Microscope and Energy-Dispersive Spectroscopy), and solid-state ^{13}C NMR spectra. The FT-IR spectra were scanned from 4000-400 cm^{-1} and collected on a Thermo Nicolet 50 spectrometer. The SEM spectra were obtained by an EVO 18 scanning electron microscope. The TEM-EDS analyses were carried out on an FEI Tecnai G2 field emission high-resolution transmission electron microscope. A Bruker Avance III 400 HD instrument with the magic-angle spinning frequency of 80 kHz was used to collect the solid-state ^{13}C NMR spectroscopy of the synthesized materials. In addition, the X-ray photoelectron spectroscopy (XPS) analysis was carried out to analyze the electronic structure of the SCU-CPN-4 and SCU-CPN-4-Re.

Section 4. Batch experiments

Typically, 10 mg of SCU-CPN-4 materials were mixed with 10 ml of ^{99}TcO$_4^-$/ReO$_4^-$ solution in a glass beaker. The mixtures were stirred at room temperature for 2 h. These mixtures were subsequently separated by a 0.22 μm nylon membrane filter (SANJIA Biochemical Supplies). The concentration of ^{99}TcO$_4^-$ in solution was determined by monitoring the activity of ^{99}TcO$_4^-$ on a liquid scintillation counting (LSC) system (Perkin Elmer Quantulus 1220). The concentration of ReO$_4^-$ in solution was measured on an inductively coupled plasma-atomic emission spectrometry (ICP-AES, Thermo Fisher Scientific iCAP 7000).

The removal rate (S%), the sorption amount (q_e (mg/g)), and the distribution coefficient (Kd) of SCU-CPN-4 were calculated via the following equations:

$$S\% = \frac{C_0 - C_e}{C_0} \times 100\% \quad (1)$$

$$q_e = \frac{(C_0 - C_e)V}{m} \quad (2)$$

$$K_d = \frac{(C_0 - C_e)V}{m\,C_e} \quad (3)$$

Where C_0 (mg/L) and C_e (mg/L) are the initial concentration and equilibrium concentration of ^{99}TcO$_4^-$/ReO$_4^-$, respectively; m/V (g/L) is the phase ratio of the uptake systems.

Sorption kinetics study. 20 mg of SCU-CPN-4 materials were mixed with 0.5 ml of water and treated with ultrasound for 10 min, then the mixture was added to 20 ml of 0.15 mmol/L ^{99}TcO$_4^-$ or ReO$_4^-$ solution in a beaker, the mixture was separated and analyzed after being stirred for a certain time (1 min, 3min, 6 min, 10 min, and 20 min). Besides, the sorption kinetics of SCU-CPN-4 at a low solid/liquid ratio was carried out to further quantify the uptake kinetics, 20 mg of SCU-CPN-4 were mixed with 0.5 ml of water and treated with ultrasound for 10 min, then the mixture was added to 100 ml of ReO$_4^-$ stock solution (0.15 mmol/L) in a beaker, the mixture was separated and analyzed after stirred for a certain time (1.5 min, 3 min, 5 min, 10 min, 15 min, 20 min, 30 min, 60 min, 90 min, 120 min, and 180 min). The Pseudo-first-order and Pseudo-second-order model were used to analyze sorption kinetics. The two models are expressed as followed:

Pseudo-first-order model:

$$\ln(q_e - q_t) = \ln q_e - k_1 t \quad (4)$$

Pseudo-second-order model:

$$\frac{t}{q_t} = \frac{1}{k_2 q_e^2} + \frac{t}{q_e} \quad (5)$$

where k$_1$ (min^{-1}) and k$_2$ (g/(mg min)) are constants of Pseudo-first-order model and pseudo-second-order model, respectively. q$_t$ and q$_e$ are the sorption capacity at time t and equilibrium time, respectively.

Sorption isotherm investigations. The sorption isotherm experiments of SCU-CPN-4 for ReO$_4^-$ were carried out by mixing 10 mg of SCU-CPN-4 materials with 10 ml of a certain concentration (28 ppm, 50 ppm, 100 ppm, 200 ppm, 250 ppm, 300 ppm, 350 ppm, 400 ppm, 500 ppm, 600 ppm) of initial Re solution in a glass beaker, the samples were separated and analyzed after being stirred for 2 hours.

Two isotherm models, including Langmuir isotherm model (4) and Freundlich model (5) were used to fit the sorption data and can be expressed in the following equations:

Langmuir model:

$$\frac{C_e}{q_e} = \frac{1}{q_m K_L} + \frac{C_e}{q_m} \qquad (6)$$

Freundlich model:

$$\ln q_e = \ln K_F + \frac{1}{n} \ln C_e \qquad (7)$$

where q_m (mg/g) is the maximum sorption capacity of ReO_4^-; K_L, K_F, and n are the Langmuir constants, Freundlich constants and the sorption intensity, respectively.

Effect of pH. In this section, the pH of the solution was adjusted with NaOH and/or HNO_3 solutions in 5 min. the effect of pH for ReO_4^- sorption of SCU-CPN-4 was evaluated by adding 10 mg of SCU-CPN-4 materials to 10 ml of 28 ppm Re solution at different pH (pH= 2, 4, 6, 8, 10, 12), the samples were separated and analyzed after stirred for 2 hours.

Anion selectivity study. The effect of excessive competing NO_3^- ion was carried out by loading 10 mg of SCU-CPN-4 materials to 10 ml of a mixed solution of 28 ppm Re and a certain concentration of NO_3^- ion (0.15 mM, 1.5 mM, 15 mM, and 150 mM) in a beaker, the samples were separated and analyzed after stirred for 2 h. In addition, the influence of SO_4^{2-} ion was further explored by mixing 10 mg of SCU-CPN-4 materials with 10 ml of a mixed solution of 14 ppm Re and a certain concentration of SO_4^{2-} ion (0.075 mM, 0.75 mM, 7.5 mM, and 75 mM).

Radiation-resistance measurements. The sorption capacities of irradiated-SCU-CPN-4 were evaluated in this section. The irradiated-SCU-CPN-4 materials were obtained by irradiating the original SCU-CPN-4 powders in air at different doses (100, and 200 kGy) of β- or γ-ray. The β-ray and The γ-ray were provided by an electron irradiation accelerator device (1.5 MeV) and a ^{60}Co irradiation source, respectively. 10 mg of irradiated-SCU-CPN-4 materials were mixed with 10 ml of 500 ppm Re solution in a beaker, the samples were separated and analyzed after being stirred for 2 hours.

Anion-exchange experiments and recyclability of SCU-CPN-4 under 1 M NaOH condition. The anion-exchange experiments at 1M NaOH solution were carried out by mixing 50 mg of SCU-CPN-4 with 50 ml of 1M NaOH solutions containing 28 ppm Re. After being stirred for 2 h, the samples were separated for ICP analysis. The recyclability of SCU-CPN-4 at this condition was further evaluated by soaking SCU-CPN-4-Re powders with saturated sodium chloride (NaCl) solution three times, and then, the regenerated samples were used for ReO_4^- uptake for multiple runs. Besides, 50 mg of SCU-CPN-4, SCU-103, SCU-CPN-1, and SCU-CPN-2 were mixed with 50 ml 1M NaOH solutions, respectively. Then the mixtures were separated after being shaken at 25 °C for 24 h. The exposed SCU-CPN-4, SCU-103, SCU-CPN-1, and SCU-CPN-2 were regenerated by being soaked with 50 ml of 2 M NaCl solution, 2 M $NaNO_3$ solution, 2 M NaCl solution, and 2 M NaCl solution, respectively. The regenerated samples were further used for sorption capacity analysis.

Dynamic sorption column experiment under 1 M NaOH condition. Dynamic sorption column experiment was carried out on an auto solid-phase extraction system (SepathsUP4). In this section, 100 mg of SCU-CPN-4 were added to 1 mL of water. After treating with ultrasound for 5 min, the mixture was packed into a column for dynamic sorption of 1 M NaOH solution containing 28 ppm Re at a flow rate of 2 mL/min. After saturated sorption, the column was washed with deionized water and then recovered by contacting with 2 M NaCl solution at a flow rate of 5 mL/min for multiple runs. What's more, the dynamic sorption column experiment of SCU-103, SCU-CPN-1, and SCU-CPN-2 was analyzed under the same condition. The dynamic sorption capacity was calculated via the following equation:

$$q_e = \frac{\int_0^V (C_0 - C_V) dV}{m} \qquad (8)$$

where C_0 (mg/L) and C_e (mg/L) are the initial concentration and equilibrium concentration of ReO_4^-, respectively; m (mg) and V (mL) are the mass of the sorbent and the volume of the solution, respectively.

Anion-exchange experiments under simulated Hanford wastes. The simulated Hanford Low Activity Waste (LAW) Melter Recycle Stream was prepared according to a reported protocol[1,2]. The sorption performance of SCU-CPN-4 for $^{99}TcO_4^-$ at this simulated waste was evaluated by mixing SCU-CPN-4 materials with the simulated solution at a solid/liquid ratio of 5 g/L in a beaker, the samples were separated and analyzed after being stirred for 2 h. Besides, the sorption performance of SCU-CPN-4 for ReO_4^- was carried out under the same conditions.

Anion-exchange experiments and recyclability of SCU-CPN-4 under simulated SRS HLW Stream. The simulated SRS HLW Stream was prepared according to a reported protocol[1,2]. The sorption performance of SCU-CPN-4 for $^{99}TcO_4^-$ at this simulated waste was evaluated by mixing SCU-CPN-4 materials with the simulated solution at a solid/liquid ratio of 20 g/L in a beaker, the samples were separated and analyzed after being stirred for 2 h. Besides, the sorption performance of SCU-CPN-4 for ReO_4^- was carried out under the same conditions. The recyclability of SCU-CPN-4 for ReO_4^- at this simulated wasted was carried out by adding 200 mg of SCU-CPN-4 to 5 ml of the simulated SRS wastes containing ReO_4^-. The SCU-CPN-4 was regenerated by soaking SCU-CPN-4-Re powders with saturated sodium chloride (NaCl) solution three times, and then, the regenerated samples were used for ReO_4^- uptake for multiple runs.

Dynamic column sorption experiments under simulated SRS HLW Stream. In this section, 300 mg of SCU-CPN-4 were added to 1 ml water, after treating with ultrasound for 5 min, the mixture was packed into a column for dynamic sorption analysis with a mother solution of simulated SRS High-Level Wastes at a flow rate of 1.35 ml/min.

Section 5. Computational method

Density functional theory (DFT) calculations were performed using the Gaussian 09 program.[23] To investigate the mechanism of the remarkable alkaline-stability of SCU-CPN-4 compared with SCU-CPN-1, two fragment models, M^+ and M^{*+}, which containing their foremost structural features were constructed to simulate SCU-CPN-4 and SCU-CPN-1. The geometries of M^+ and M^{*+} were optimized at B3LYP-D3/6-31G*[24-27] level. The electrostatic potential (ESP) on the van der Waals (vdW) surfaces (isodensity = 0.001 a.u.) of M^+ and M^{*+} were calculated at M062X-D3/6-311++G**[28,29] level based on their optimized structures. The maximum values of ESP were calculated using the Multiwfn program[30]. To study the thermal vibrational behavior of M^+ fragment, we performed a 2000 fs molecular dynamics (MD) simulation by xTB (extended tight binding) program[31] at 298.15 K. The structures of M^+ were extracted from the MD trajectory every 4 fs. For M^+/M^{*+}-Anion (Anion = NO_3^-, SO_4^{2-} and TcO_4^-) complex structures, geometries were optimized at B3LYP-D3/6-31G* level. The Stuttgart/Dresden relativistic effective core potentials (SDD) and corresponding valence basis sets[32] were applied for the Re atom. Based on the optimized reactant and product, single-point energies were then performed at different levels for calculating different terms of ΔH. The values of ΔH were calculated by

$$\Delta H = H_{product} - H_{reactant}$$

$H = \varepsilon_{ele} + \Delta G_{solv} + H_{corr}$

$\Delta G_{solv} = E_{sol} - E_{gas} + 1.89$ kcal/mol

where ε_{ele} is the high-precision electronic energy calculated at M062X-D3/6-311++G** level. ΔG_{solv} is the solvation free energy. E_{sol} and E_{gas} are single-point energies in the liquid phase and gas phase calculated at the B3LYP-D3/6-31G* level. For E_{sol}, the PCM[33] implicit solvent model was used. H_{corr} is a correction term to enthalpy calculated at the B3LYP-D3/6-31G* level. All the figures of molecular structures were plotted by VMD[34] software.

Table S1. Comparison of the equilibrium time and rate constant of SCU-CPN-4 with other cationic materials.

Sorbents	Experimental conditions	Equilibrium time	Ref.
SBN	$[Re]_0 = 28$ mg/L; pH = 7; 0.5 g/L; stirring	10 min	3
PAF-1-F	Molar ratio ReO_4^-: PAF-1-F = 1:2	250 min	4
SCU-100	$[Re]_0 = 28$ mg/L; pH = 7; 1 g/L; stirring	30 min	1
Acidosasa edulis shoot shell bio-char	T = 298 K; pH = 1; 3 g/L; $[Re]_0 = 20$ mg/L	350 min	5
PS-g-4VP-IE	$[Re]_0 = 2000$ mg/L; V = 5 ml; $m_{sorbent} = 0.1$g; T = 298 K	30 min	6
PP-g-2-VP	$[Re]_0 = 320$ mg/L; pH = 2.2	30 min	7
ZrO2@rGO	pH = 4.0 ± 0.1; 0.1 mg/L; $[Re]_0 = 10.00$ mg/L; T = 293 K	5 h	8
rGOs	0.1 g/L; $[Re]_0 = 20.0$ mg/L; pH = 3.0	10 min	9
NZVI	0.1 g/L; $[Re]_0 = 20.0$ mg/L; pH = 3.0	90 min	9
NZVI/rGOs	0.1 g/L; $[Re]_0 = 20.0$ mg/L; pH = 3.0	50 min	9
4-ATR resin	$m_{sorbent} = 10.0$ mg; $[Re]_0 = 7.2$ mg/50.0 mL; pH = 2.6; 100 rpm	8 h	10
R2SO4 resin	$[Re]_0 = 200$ mg/L, V = 15 mL; $m_{sorbent} = 0.02$ g; pH = 6.25; room temperature	60 min	11
D318 Resin	$m_{sorbent} = 50.0$ mg; $[Re]_0 = 320$ mg/L; T = 298 K; V = 50.0 mL	115 min	12
Purolite A532E	$[Re]_0 = 28$ mg/L; pH = 7; 1 g/L; stirring	150 min	13
Purolite A530E	$[Re]_0 = 28$ mg/L; pH = 7; 1 g/L; stirring	150 min	13
UiO-66-NH3+	molar ratio ReO_4^-/ UiO-66-NH_3^+ = 1:2	>24 h	14
SCU-101	$[Re]_0 = 28$ mg/L; pH = 7; 1 g/L; stirring	10 min	15
SCU-CPN-1	$[Re]_0 = 28$ mg/L; pH = 7; 1 g/L; stirring	30 s	16
DhaTGCl	T=298 K; 1 g/L	5 min	17
SCU-COF-1	$[Re]_0 = 28$ mg/L; pH = 7; 1 g/L	1 min	18
SCU-CPN-4	$[Re]_0 = 28$ mg/L; pH = 7; 1 g/L	1 min	This work

Table S2. Fitting results based on Pseudo-first-order and Pseudo-second-order model

Sample	Pseudo-first-order			Pseudo-second-order		
	k_1(min^{-1})	q_e (mg g^{-1})	R^2	k_2(g mg^{-1} min^{-1})	q_e (mg g^{-1})	R^2
SCU-CPN-4	3.90×10^{-2}	29.66	0.76	5.60×10^{-3}	184.16	>0.99

Table S3. Fitting results based on the Langmuir and Freundlich models.

Sample	Langmuir			Freundlich		
	q_m (mg g^{-1})	K_L (L mg^{-1})	R^2	k_F (L^n/mol^{n-1} g)	n	R^2
SCU-CPN-4	437	2.43	>0.98	232	7.72	0.80

Table S4. Comparison of the sorption capacities of SCU-CPN-4 with other cationic materials.

Sorbents	Experimental conditions	Capacity (mg/g)	Ref.
Nano SiO$_2$	T=298 K; pH 2	4.94	19
Yb$_3$O(OH)$_6$Cl	Ambient temperature; pH=7.0±0.1; 0.5 g/L	48.6	3
NDTB-1	Ambient temperature; pH=7.0±0.1; 0.5 g/L	49.4	3
LDHs	Ambient temperature; pH=7.0±0.1; 0.5 g/L	130.2	3
ZrO$_2$@rGO	T=303 K; 24 h	43.55	8
ZBC	T=298 K; 3 g/L; pH 1	25.92	20
NZVI/rGOs	0.1 g/L; pH 5	85.77	9
GO-DEA-DIBA	303 K; 2 g/L; 48 h	140.82	21
PP-g-2-VP	pH 2.2; appropriate temperature	113	7
PS-g-4VP-IE	Ambient temperature; 2 h	252	6
D318 resin	T=298 K; pH 5.2; 1 g/L	351	12
4-ATR resin	T=298 K; 8 h; pH 2.6	354	10
UiO-66-NH$_3$$^+$	24 h	159	14
TJNU-302	Room temperature	211	19
SCU-101	Ambient temperature; pH=7.0±0.1; 1 g/L	217	15
SCU-102	Ambient temperature; pH=7.0±0.1; 1 g/L	291	22
SCU-CPN-4	Ambient temperature; pH=7.0±0.1; 1 g/L	437	This work

Table S5. Comparison of the distribution coefficient (K_d) With other cationic materials.

Cationic materials	K_d (ml g^{-1})	Ref.
Mg-Al-LDH	262	15
NDTB-1	652	15
Y$_2$(OH)$_5$Cl	112	15
Yb$_3$O(OH)$_6$Cl	120	15
PAF-1-F	2.55×10^4	4
SCU-6	3.0×10^3	1
SCU-100	3.3×10^5	1
SCU-102	5.6×10^5	22
SCU-CPN-1	6.2×10^5	16
Purolite A530E	7.6×10^5	13
PQA-pN(Me)2Py-Cl	1×10^7	2
SCU-CPN-4	1.5×10^7	This work

Table S6. Composition of Hanford Low Activity Waste (LAW) Melter Recycle Stream.

Anions	Concentration (mol/L)	Molar ratio (Anion: TcO$_4^-$)
TcO$_4^-$	1.94×10^{-4}	1.0
NO$_3^-$	6.07×10^{-2}	314
Cl$^-$	6.39×10^{-2}	330
NO$_2^-$	1.69×10^{-1}	873
SO$_4^{2-}$	6.64×10^{-6}	0.0343
CO$_3^{2-}$	4.30×10^{-5}	0.222

Table S7. Composition of Savannah River Site (SRS) High-Level Waste (HLW) Stream.

Anions	Concentration (mol/L)	Anion:TcO_4^- molar ratio
ReO_4^-/TcO_4^-	7.92×10^{-5}	1.0
NO_3^-	2.6	32819
OH^-	1.33	16788
NO_2^-	1.34×10^{-1}	1691
SO_4^{2-}	6.64×10^{-6}	6576
CO_3^{2-}	4.30×10^{-5}	328

Table S8. Results of ReO_4^- sorption by SCU-CPN-4 in simulated Hanford waste and SRS waste.

Simulated wastes	Anions	Solid-to-liquid ratio	Anion removal
Hanford waste	ReO_4^-	5:1	90.7
	TcO_4^-	5:1	97.4
SRS waste	ReO_4^-	20:1	86.2
	ReO_4^-	40:1	92.1
	TcO_4^-	20:1	94.3
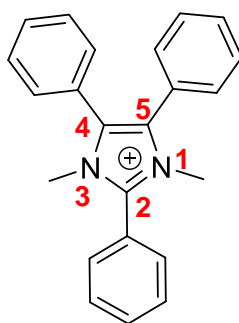
Figure S1. The model for describing the local structure of SCU-CPN-4.
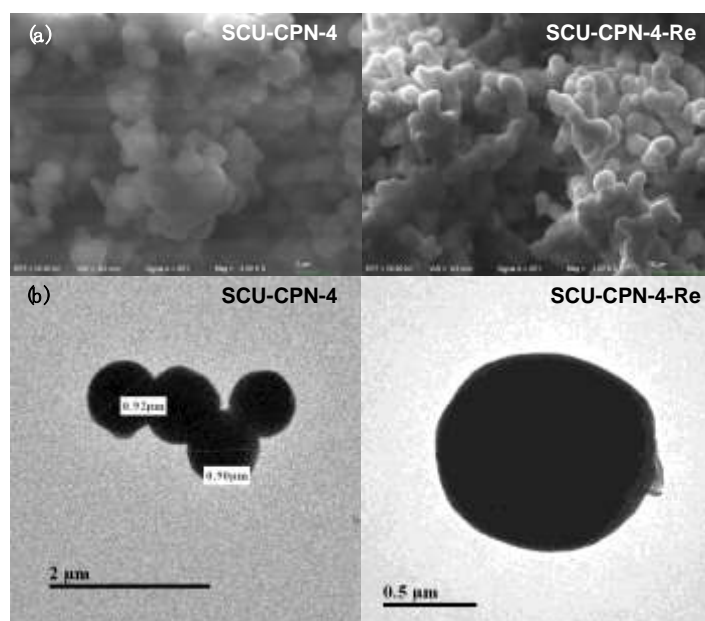

Figure S2. (a) SEM analysis of SCU-CPN-4 and SCU-CPN-4-Re. (b) TEM analysis of SCU-CPN-4 and SCU-CPN-4-Re.
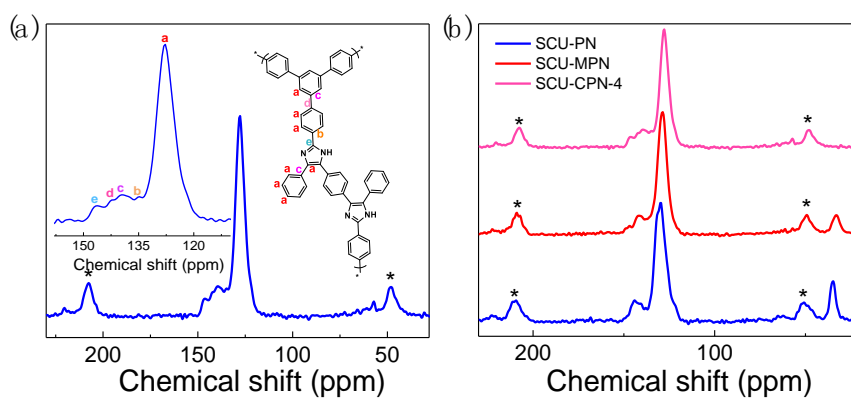

Figure S3. (a) Solid-state ^{13}C NMR spectrum of SCU-PN. (b) Solid-state ^{13}C NMR spectrum of SCU-PN, SCU-MPN, and SCU-CPN-4.
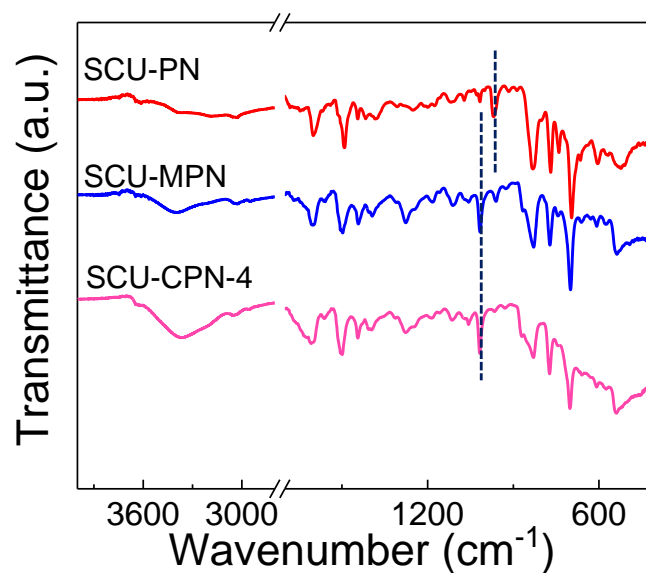
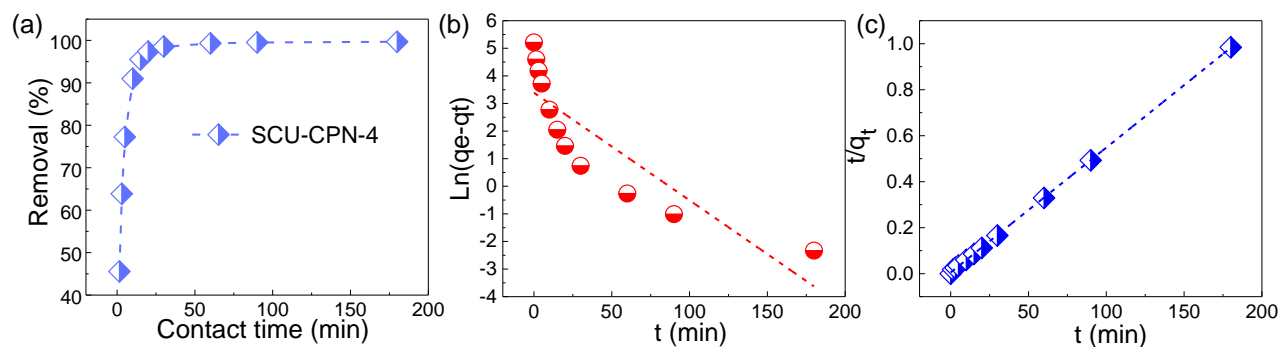Figure S4. FT-IR spectra of SCU-PN, SCU-MPN, and SCU-CPN-4.

Figure S5. (a) Sorption kinetics of ReO$_4^-$ by SCU-CPN-4. Conditions: [Re]$_{initial}$ = 28 ppm and m$_{sorbent}$/V$_{solution}$ = 0.2 g/L. (b) Pseudo-first-order model and (c) Pseudo-second-order model for ReO$_4^-$ by SCU-CPN-4.

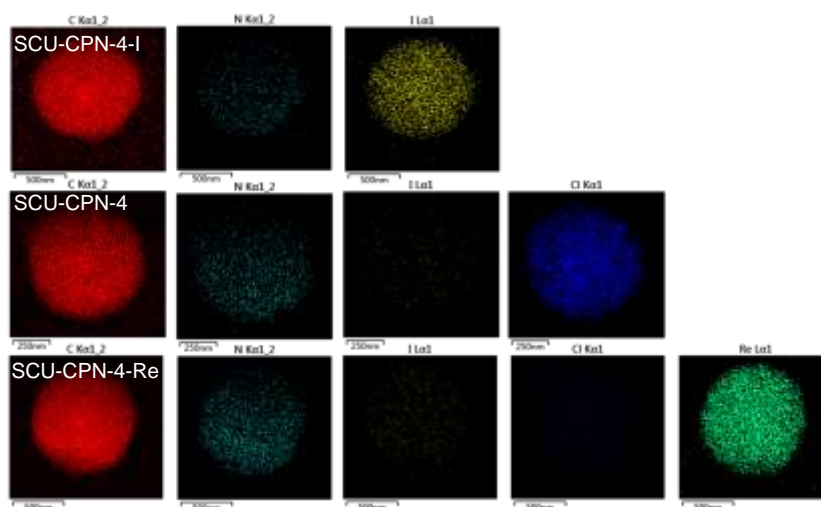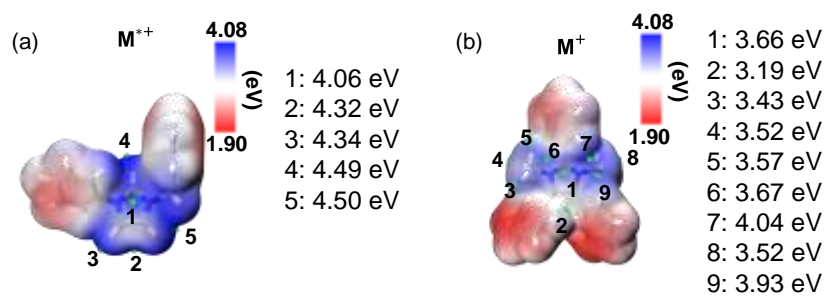Figure S6. TEM-EDS mapping of SCU-CPN-4-I, SCU-CPN-4, and SCU-CPN-4-Re.

(a) M*+

4.08

(eV)

1.90

4
1
5
3 2

1: 4.06 eV
2: 4.32 eV
3: 4.34 eV
4: 4.49 eV
5: 4.50 eV

(b) M+

4.08

(eV)

1.90

5 6 7
4   8
3   1   9
2

1: 3.66 eV
2: 3.19 eV
3: 3.43 eV
4: 3.52 eV
5: 3.57 eV
6: 3.67 eV
7: 4.04 eV
8: 3.52 eV
9: 3.93 eV

Figure S7. The ESP maxima values near the imidazole ring of (a) M*+ and (b) M+.

References

(1) Sheng, D.; Zhu, L.; Xu, C.; Xiao, C.; Wang, Y.; Wang, Y.; Chen, L.; Diwu, J.; Chen, J.; Chai, Z.; Albrecht-Schmitt, T. E.; Wang, S. Efficient and Selective Uptake of TcO_4^- by a Cationic Metal-Organic Framework Material with Open Ag^+ Sites. *Environ. Sci. Technol.* 2017, *51*, 3471-3479.

(2) Sun, Q.; Zhu, L.; Aguila, B.; Thallapally, P. K.; Xu, C.; Chen, J.; Wang, S.; Rogers, D.; Ma, S. Optimizing radionuclide sequestration in anion nanotraps with record pertechnetate sorption. *Nat. Commun.* 2019, *10*, 1646.

(3) Zhu, L.; Xiao, C.; Dai, X.; Li, J.; Gui, D.; Sheng, D.; Chen, L.; Zhou, R.; Chai, Z.; Albrecht-Schmitt, T. E.; Wang, S. Exceptional Perrhenate/Pertechnetate Uptake and Subsequent Immobilization by a Low-Dimensional Cationic Coordination Polymer: Overcoming the Hofmeister Bias Selectivity. *Environ. Sci. Technol. Lett.* 2017, *4*, 316-322.

(4) Banerjee, D.; Elsaidi, S. K.; Aguila, B.; Li, B.; Kim, D.; Schweiger, M. J.; Kruger, A. A.; Doonan, C. J.; Ma, S.; Thallapally, P. K. Removal of Pertechnetate-Related Oxyanions from Solution Using Functionalized Hierarchical Porous Frameworks. *Chemistry* 2016, *22*, 17581-17584.

(5) Hu, H.; Jiang, B.; Zhang, J.; Chen, X. Adsorption of perrhenate ion by bio-char produced from Acidosasa edulis shoot shell in aqueous solution. *RSC Adv.* 2015, *5*, 104769-104778.

(6) Zu, J.; Ye, M.; Wang, P.; Tang, F.; He, L. Design of a strong-base anion exchanger and its adsorption and elution behavior for rhenium(VII). *RSC Adv.* 2016, *6*, 18868-18873.

(7) Zu, J.; Wei, Y.; Ye, M.; Tang, F.; He, L.; Lui, R. Preparation of a new anion exchanger by pre-irradiation grafting technique and its adsorptive removal of rhenium (VII) as analogue to ^{99}Tc. *Nucl. Sci. Tech.* 2015, *26*, 69-75.

(8) Gao, Y.; Chen, K.; Tan, X.; Wang, X.; Alsaedi, A.; Hayat, T.; Chen, C. Interaction Mechanism of Re(VII) with Zirconium Dioxide Nanoparticles Archored onto Reduced Graphene Oxides. *ACS Sustain. Chem. Eng.* 2017, *5*, 2163-2171.

(8) Li, J.; Chen, C.; Zhang, R.; Wang, X. Reductive immobilization of Re(VII) by graphene modified nanoscale zero-valent iron particles using a plasma technique. *Sci. China Chem.* 2015, *59*, 150-158.

(10) Xiong, C.; Yao, C.; Wu, X. Adsorption of rhenium(VII) on 4-amino-1,2,4-triazole resin. *Hydrometallurgy* 2008, *90*, 221-226.

(11) Jia, M.; Cui, H.; Jin, W.; Zhu, L.; Liu, Y.; Chen, J. Adsorption and separation of rhenium(VII) using N-methylimidazolium functionalized strong basic anion exchange resin. *J. Chem. Technol. Biot. 2*013, *88* (3), 437-443.

(12) Shu, Z.; Yang, M. Adsorption of rhenium(vii) with anion exchange resin D318 *Chinese J. Chem. Eng.* 2010, *18*, 372-376.

(13) Li, J.; Zhu, L.; Xiao, C.; Chen, L.; Chai, Z.; Wang, S. Efficient uptake of perrhenate/pertechnenate from aqueous solutions by the bifunctional anion-exchange resin. *Radiochim. Acta* 2018, *106*, 581-591.

(14) Banerjee, D.; Xu, W.; Nie, Z.; Johnson, L. E.; Coghlan, C.; Sushko, M. L.; Kim, D.; Schweiger, M. J.; Kruger, A. A.; Doonan, C. J.; Thallapally, P. K. Zirconium-Based Metal-Organic Framework for Removal of Perrhenate from Water. *Inorg. Chem.* 2016, *55*, 8241-8243.

(15) Zhu, L.; Sheng, D.; Xu, C.; Dai, X.; Silver, M. A.; Li, J.; Li, P.; Wang, Y.; Wang, Y.; Chen, L.; Xiao, C.; Chen, J.; Zhou, R.; Zhang, C.; Farha, O. K.; Chai, Z.; Albrecht-Schmitt, T. E.; Wang, S. Identifying the Recognition Site for Selective Trapping of $^{99}TcO_4^-$ in a Hydrolytically Stable and Radiation Resistant Cationic Metal-Organic Framework. *J. Am. Chem. Soc.* 2017, *139*, 14873-14876.

(16) Li, J.; Dai, X.; Zhu, L.; Xu, C.; Zhang, D.; Silver, M. A.; Li, P.; Chen, L.; Li, Y.; Zuo, D.; Zhang, H.; Xiao, C.; Chen, J.; Diwu, J.; Farha, O. K.; Albrecht-Schmitt, T. E.; Chai, Z.; Wang, S. $^{99}TcO_4^-$ remediation by a cationic polymeric network. *Nat. Commun.* 2018, *9*, 3007.

(17) Da, H. J.; Yang, C. X.; Yan, X. P. Cationic Covalent Organic Nanosheets for Rapid and Selective Capture of Perrhenate: An Analogue of Radioactive Pertechnetate from Aqueous Solution. *Environ. Sci. Technol.* 2019, *53*, 5212-5220.

(18) He, L.; Liu, S.; Chen, L.; Dai, X.; Li, J.; Zhang, M.; Ma, F.; Zhang, C.; Yang, Z.; Zhou, R.; Chai, Z.; Wang, S. Mechanism unravelling for ultrafast and selective $^{99}TcO_4^-$ uptake by a radiation-resistant cationic covalent organic framework: a combined radiological experiment and molecular dynamics simulation study. *Chem. Sci.* 2019, *10*, 4293-4305.

(19) Li, Y.; Wang, Q.; Li, Q.; Zhang, Z.; Zhang, L.; Liu, X. Simultaneous speciation of inorganic rhenium and molybdenum in the industrial wastewater by amino-functionalized nano-SiO_2. *J. Taiwan Inst. Chem. Eng.* 2015, *55*, 126-132.

(20) Hu, H.; Sun, L.; Gao, Y.; Wang, T.; Huang, Y.; Lv, C.; Zhang, Y. F.; Huang, Q.; Chen, X.; Wu, H. Synthesis of ZnO nanoparticle-anchored biochar composites for the selective removal of perrhenate, a surrogate for pertechnetate, from radioactive effluents. *J. Hazard. Mater.* 2020, *387*, 121670.

(21) Xiong, Y.; Cui, X.; Zhang, P.; Wang, Y.; Lou, Z.; Shan, W. Improving Re(VII) Adsorption on Diisobutylamine-Functionalized Graphene Oxide. *ACS Sustain. Chem. Eng.* 2016, *5*, 1010-1018.

(22) Sheng, D.; Zhu, L.; Dai, X.; Xu, C.; Li, P.; Pearce, C. I.; Xiao, C.; Chen, J.; Zhou, R.; Duan, T.; Farha, O. K.; Chai, Z.; Wang, S. Successful Decontamination of $^{99}TcO_4^-$ in Groundwater at Legacy Nuclear Sites by a Cationic Metal-Organic Framework with Hydrophobic Pockets. *Angew. Chem., Int. Ed.* 2019, *58*, 4968-4972.

(23) Gaussian 09, Revision E.01, M. J. Frisch, G. W. Trucks, H. B. Schlegel, G. E. Scuseria, M. A. Robb, J. R. Cheeseman, G. Scalmani, V. Barone, B. Mennucci, G. A. Petersson, H. Nakatsuji, M. Caricato, X. Li, H. P. Hratchian, A. F. Izmaylov, J. Bloino, G. Zheng, J. L. Sonnenberg, M. Hada, M. Ehara, K. Toyota, R. Fukuda, J. Hasegawa, M. Ishida, T. Nakajima, Y. Honda, O. Kitao, H. Nakai, T. Vreven, J. A. Montgomery, Jr., J. E. Peralta, F. Ogliaro, M. Bearpark, J. J. Heyd, E. Brothers, K. N. Kudin, V. N. Staroverov, R. Kobayashi, J. Normand, K. Raghavachari, A. Rendell, J. C. Burant, S. S. Iyengar, J. Tomasi, M. Cossi, N. Rega, J. M. Millam, M. Klene, J. E. Knox, J. B. Cross, V. Bakken, C. Adamo, J. Jaramillo, R. Gomperts, R. E. Stratmann, O. Yazyev, A. J. Austin, R. Cammi, C. Pomelli, J. W. Ochterski, R. L. Martin, K. Morokuma, V. G. Zakrzewski, G. A. Voth, P. Salvador, J. J. Dannenberg, S. Dapprich, A. D. Daniels, Ö. Farkas, J. B. Foresman, J. V. Ortiz, J. Cioslowski, and D. J. Fox, Gaussian, Inc., Wallingford CT, 2009.

(24) Lee, C.; Yang, W.; Parr, R. G. Development of the Colle-Salvetti correlation-energy formula into a functional of the electron density. *Phys. Rev. B: Condens. Matter Mater. Phys.* 1988, *37*, 785-789.

(25) Becke, A. D. Density-functional thermochemistry. III. The role of exact exchange. *J. Chem. Phys.* 1993, *98*, 5648-5652.

(26) Hehre, W. J.; Ditchfield, R.; Pople, J. A. Self-consistent molecular orbital methods. xii. further extensions of gaussia-type basis sets for use in molecular orbital studies of organic molecules. *J. Chem. Phys.* 1972, *56*, 2257-2261.

(27) Grimme, S.; Antony, J.; Ehrlich, S.; Krieg, H. A consistent and accurate ab initio parametrization of density functional dispersion correction (DFT-D) for the 94 elements H-Pu. *J. Chem. Phys.* 2010, *132*, 154104.

(28) Zhao, Y.; Truhlar, D. G. The M06 suite of density functionals for main group thermochemistry, thermochemical kinetics, noncovalent interactions, excited states, and transition elements: two new functionals and systematic testing of four M06-class functionals and 12 other functionals. *Theor. Chem. Acc.* 2008, *120*, 215–241.

(29) Clark, T.; Chandrasekhar, J.; Spitznagel, G. W.; Schleyer, P. V. R. Efficient diffuse function-augmented basis sets for anion calculations. III. The 3-21+G basis set for first-row elements, Li-F. *J. Comput. Chem.* 1983, *4*, 294-301.

(30) Lu, T.; Chen, F. Multiwfn: A multifunctional wavefunction analyzer. *J. Comput. Chem.* 2012, *33*, 580-592.

(31) Grimme, S.; Bannwarth, C.; Shushkov, J. P. A robust and accurate tight-binding quantum chemical method for structures, vibrational frequencies, and noncovalent interactions of large molecular systems parametrized for all spd-block elements (Z = 1–86). *Chem. Theory Comput.* 2017, *13*, 1989-2009.

(32) Andrae, D.; Häußermann, U.; Dolg, M.; Stoll, H.; Preuß, H. Energy-adjusted ab initio pseudopotentials for the second and third row transition elements. *Theoret. Chim. Acta* 1990, *77*, 123-141.

(33) Miertus, S.; Scrocco, E.; Tomasi, J. Electrostatic interaction of a solute with a continuum. A direct utilizaion of AB initio molecular potentials for the prevision of solvent effects. *Chem. Phys.* 1981, *55*, 117-129.

(34) Humphrey, W. Dalke, A. Schulten, K. VMD: visual molecular dynamics. *J. Mol.Graph. Model.* 1996, *14*, 33-38.

12